# UC Santa Barbara
## UC Santa Barbara Previously Published Works

**Title**
WIDE AWAKE mediates the circadian timing of sleep onset.

**Permalink**
https://escholarship.org/uc/item/4j9709cm

**Journal**
Neuron, 82(1)

**ISSN**
0896-6273

**Authors**
Liu, Sha
Lamaze, Angelique
Liu, Qili
et al.

**Publication Date**
2014-04-01

**DOI**
10.1016/j.neuron.2014.01.040

**Copyright Information**

Peer reviewed

# WIDE AWAKE Mediates the Circadian Timing of Sleep Onset

**Sha Liu**[1,7], **Angelique Lamaze**[2,7], **Qili Liu**[1], **Masashi Tabuchi**[1], **Yong Yang**[2], **Melissa Fowler**[3], **Rajnish Bharadwaj**[1], **Julia Zhang**[1], **Joseph Bedont**[4], **Seth Blackshaw**[4], **Thomas E. Lloyd**[1,4], **Craig Montell**[5], **Amita Sehgal**[6], **Kyunghee Koh**[2,8,*], and **Mark N. Wu**[1,4,8,*]

[1]Department of Neurology, Johns Hopkins University, Baltimore, MD 21287, USA

[2]Department of Neuroscience and the Farber Institute for Neurosciences, Thomas Jefferson University, Philadelphia, PA 19107, USA

[3]Department of Biological Chemistry, Johns Hopkins University, Baltimore, MD 21287, USA

[4]Department of Neuroscience, Johns Hopkins University, Baltimore, MD 21287, USA

[5]Neuroscience Research Institute and Department of Molecular, Cellular, & Developmental Biology, University of California, Santa Barbara, Santa Barbara, CA 93106, USA

[6]Howard Hughes Medical Institute, Department of Neuroscience, University of Pennsylvania, Philadelphia, PA 19104, USA

## SUMMARY

How the circadian clock regulates the timing of sleep is poorly understood. Here, we identify a *Drosophila* mutant, *wide awake* (*wake*), that exhibits a marked delay in sleep onset at dusk. Loss of WAKE in a set of arousal-promoting clock neurons, the large ventrolateral neurons (l-LNvs), impairs sleep onset. WAKE levels cycle, peaking near dusk, and the expression of WAKE in l-LNvs is *Clock* dependent. Strikingly, *Clock* and *cycle* mutants also exhibit a profound delay in sleep onset, which can be rescued by restoring WAKE expression in LNvs. WAKE interacts with the GABA$_A$ receptor Resistant to Dieldrin (RDL), upregulating its levels and promoting its localization to the plasma membrane. In *wake* mutant l-LNvs, GABA sensitivity is decreased and excitability is increased at dusk. We propose that WAKE acts as a clock output molecule specifically for sleep, inhibiting LNvs at dusk to promote the transition from wake to sleep.

## INTRODUCTION

Sleep is an essential, evolutionarily conserved behavior that is regulated by two independent processes: a circadian clock that regulates the timing of sleep and a homeostatic mechanism that influences the amount and depth of sleep (Borbély and Achermann, 1999). The core

circadian oscillator comprises a transcriptional/translational feedback loop consisting of transcriptional activators, e.g., Clock (CLK) and Cycle (CYC) or BMAL1/NPAS2, and transcriptional repressors, e.g., Period (PER) and Timeless (TIM) or Cryptochrome (CRY) (Allada and Chung, 2010; Lowrey and Takahashi, 2011). Various rhythmic behaviors are regulated by the circadian oscillator, and the timing of sleep can be considered an output of the circadian clock. Indeed, lesioning the mammalian central clock, the suprachiasmatic nucleus (SCN), or genetic ablation of core clock proteins abolishes circadian patterns of sleep under constant conditions (Eastman et al., 1984; Shaw et al., 2002; Shiromani et al., 2004). In addition, mutations in the core clock protein *Period2* (*PER2*) and *Casein Kinase 1δ* (*CK1δ*) alter the timing of sleep in humans, resulting in Familial Advanced Sleep Phase syndrome (Toh et al., 2001; Xu et al., 2005).

Despite specific progress in our understanding of the molecular clock, the mechanisms by which the circadian clock regulates sleep are poorly understood. The discovery that *Drosophila* sleep (Hendricks et al., 2000; Shaw et al., 2000) has opened the possibility for applying powerful forward genetic approaches to identify novel molecules that regulate sleep (Cirelli et al., 2005; Koh et al., 2008; Rogulja and Young, 2012; Wu et al., 2008). Here, using this approach, we identify a conserved molecule named WIDE AWAKE (WAKE), which we propose acts downstream of the circadian clock to regulate the timing of sleep onset. We find that WAKE is expressed cyclically in a CLK-dependent fashion in arousal-promoting LNv clock neurons. WAKE levels peak near the wake/sleep transition in the early night, and loss of WAKE specifically in large LNvs (l-LNvs) acts through PDF to delay sleep onset. This impairment in the timing of sleep onset is also seen in *Clk* and *cyc* mutants, which can be rescued by restoring WAKE expression in LNvs of these mutants. WAKE interacts with Resistant to Dieldrin (RDL, a GABA$_A$ receptor) and increases the expression of RDL in both heterologous cells and LNvs. Moreover, in *wake* mutants, the l-LNvs are hyperexcitable and their GABA sensitivity is reduced at dusk, supporting a function for WAKE in silencing this arousal circuit in the early night. Importantly, *wake* mutants have normal circadian rhythms of locomotor activity; thus, these data identify a molecular output of the circadian clock that specifically modulates the timing of sleep. Intriguingly, our data demonstrate that the putative mouse homolog of WAKE is enriched in the SCN, suggesting that WAKE function is conserved in mammals. Our results suggest a model whereby the circadian clock acts through WAKE to regulate sleep onset by upregulating RDL in l-LNvs in the early night, thus inhibiting the excitability of this arousal circuit and promoting sleep.

## RESULTS

### Identification and Phenotypic Analysis of *wide awake*

From a forward genetic screen of ~3,500 transposon lines (Koh et al., 2008), we identified a mutant, *wide awake* (*wake*), with significantly reduced sleep amount and markedly increased sleep latency. We named the original insertion *wake^{P1}* and obtained an additional insertion in an adjacent exon. Because this second insertion is associated with a small deletion removing the majority of that exon (see below), we refer to this allele as *wake^{D1}*. Female *wake^{D1}* and *wake^{P1}* mutants exhibited significant reductions in daily sleep, relative to background controls (Figures 1A and 1B). In addition, *wake^{D1}* failed to complement *wake^{P1}* (Figure 1B), indicating that these mutations affect the same gene. This reduction of sleep amount is not due to hyperactivity, because waking activity (activity counts per minute awake) was not increased in these *wake* mutants (Figure 1C). Although female *wake* mutants had significantly reduced sleep bout duration (Figure 1D), they did not exhibit a significant compensatory increase in sleep bout number (Figure 1E), as seen with other short-sleeping mutants (Cirelli et al., 2005; Rogulja and Young, 2012; Stavropoulos and

Young, 2011). Similar data were observed for *wake* males, except that sleep bout number was increased compared to controls (Figures S1A–S1D available online).

Most strikingly, sleep latency (defined as the duration between lights off to the first sleep bout) in *wake* mutants was markedly increased relative to background controls (Figures 1F and S1E). This phenotype, which suggests that *wake* mutants have difficulty falling asleep after lights off, was not simply due to an overall decrease in sleep, because it was not observed in another mutant with a greater reduction in sleep amount, *fumin* (*fmn*) (Figure 1F). To rule out the possibility that the increased sleep latency seen in *wake* mutants was caused by an enhanced startle response to lights off, we examined sleep in *wake*$^{D1}$ flies in constant darkness (DD). The reduced sleep amount and increased sleep latency in *wake*$^{D1}$ flies persisted in DD (Figures 1G and 1H). Thus, WAKE appears to be critical for the timing of sleep onset, although *wake* mutants do eventually fall asleep, which probably reflects the dependence of sleep onset on other factors such as accrual of sleep debt.

We next assessed circadian activity rhythm phenotypes of *wake* mutants in DD. *wake*$^{D1}$ flies did not exhibit a significant change in period length or rhythm strength (Figure 1I; Table S1) in DD, suggesting that their increased sleep latency is not due to a longer period length. *wake*$^{D1}$ flies also did not show reduced sleep rebound compared to controls (Figures 1J and 1K), demonstrating that homeostatic regulation of sleep is intact. We also examined other general behavioral phenotypes of *wake* mutants and found that phototaxis, negative geotaxis, and feeding behavior were similar to controls (Figures S1F–S1H). However, similar to most short-sleeping mutants, *wake* mutants did have a shorter lifespan than controls (Figure S1I). Together, these data suggest that *wake* mutants are not only short sleeping, but also have a pronounced delay in transitioning from wakefulness to sleep following lights off.

## Molecular Cloning of *wide awake*

The *wake*$^{P1}$ and *wake*$^{D1}$ mutants carry P element insertions (EY02219 and GS17103, respectively) in a predicted gene designated *CG42686* by the *Drosophila* Genome Project. In addition, *wake*$^{D1}$ carries an ~1 kb deletion including the fifth coding exon of *CG42686* (Figure 2A). To test the hypothesis that the sleep phenotype of *wake* mutants maps to this locus, we generated an additional allele (*wake*$^{D2}$) using FLP/FRT mitotic recombination (Parks et al., 2004) that deletes the entire *CG42686* ORF (Figure 2A). As expected, homozygous *wake*$^{D2}$ flies also exhibited significantly reduced sleep amount and increased sleep latency relative to background controls (Figures 2D and 2E). Furthermore, precise excision of the P element in *wake*$^{P1}$ mutants rescued the reduced sleep and increased sleep latency observed in these mutants (Figures 2D and 2E).

Interestingly, however, our data suggest that *CG42686* is part of a larger gene, which includes sequence from the neighboring predicted gene *CG6954* (Figure 2A). First, according to the modENCODE transcript splicing database (Roy et al., 2010), there is a splicing event between the last exon of *CG42686* and the predicted fourth coding exon of *CG6954*, which we confirmed by RT-PCR. The transcript spanning both predicted genes will be referred to as the full-length (FL) transcript. Second, we generated two antibodies: WAKE-Ab1 against the CG42686 protein and WAKE-Ab2 against a portion of the CG6954 protein. Both antibodies recognized an ~180 kDa band (the size predicted by the *wake-FL* transcript) in control head extracts, which was undetectable in *wake* mutant extracts (Figures 2B and 2C). In contrast, WAKE-Ab1 did not detect a 58 kDa band, the size predicted for CG42686 alone (Figure 2B). FlyBase predicts the presence of four *CG6954* splice variants that do not contain sequence from *CG42686* (Figure S2). However, we were unable to detect smaller bands that would correspond to the CG6954- specific isoforms (Figure 2C) in adult heads, although we cannot rule out the possibility that these isoforms are expressed at low

levels. We next generated a *wake-FL*-specific microRNA transgenic line (*UAS-wake-miR1*) (Chen et al., 2007), whose hairpins were designed to bind the fourth and fifth coding exons of *CG42686*. Panneuronal expression of this micro-RNA using *nsyb-Gal4* rendered WAKE expression undetectable (Figure S2B) and recapitulated the *wake* mutant phenotype, suggesting that knockdown of the *wake-FL* isoform alone is sufficient to cause the mutant phenotype (Figures 2D and 2E). Together, these data strongly suggest that the sleep phenotype in *wake* mutants is caused by disruption of this 180 kDa protein, which consists of sequence from both *CG42686* and *CG6954*, and henceforth we will refer to this full-length protein as WAKE. WAKE consists of a large N-terminal unstructured domain, two ankyrin repeats, a fibronectin type III domain, and a ubiquitin-like fold. Unstructured domains often promote flexible binding with multiple partners, and the other domains are common protein-protein interaction motifs (Dyson and Wright, 2005; Mosavi et al., 2004). We next asked whether overexpressing WAKE specifically during the adult stage would increase sleep. We generated *UAS-wake* flies and drove WAKE expression with the drug-inducible panneuronal *elav-Geneswitch* driver (Osterwalder et al., 2001). Flies in which WAKE overexpression was induced by ingested RU486 exhibited a significant increase in sleep amount and decrease in sleep latency, compared to vehicle-fed control flies (Figures 2F–2H). These data are consistent with our loss-of-function data (Figures 2D and 2E) and further support a role for WAKE in promoting sleep.

### WIDE AWAKE Is Expressed in Clock Neurons and Is Specifically Required in Large LNv Cells to Regulate Sleep Onset

To examine where WAKE is expressed in the adult brain, we generated transgenic flies (*wake-Gal4*) carrying ~4.5 kb of genomic sequence upstream of the *wake* translational start site fused to GAL4, as both WAKE antibodies did not work for immunostaining. When *wake-Gal4* was used to drive *UAS-CD8:: GFP*, GFP expression was seen in a limited number of neurons in the central brain (Figures 3A and 3B). Knockdown of WAKE using *wake-Gal4* to drive *UAS-wake-miR1* reproduced the *wake* sleep phenotype, i.e., increased sleep latency and decreased sleep time, suggesting that *wake-Gal4* drives expression in most of the WAKE+ cells important for sleep regulation (Figures 3D and 3E).

Strikingly, the *wake-Gal4* expression pattern includes subsets of clock neurons (Figure 3C; Figures S3A and S3B), as determined by colocalization with PER. These clock neurons include all pigment-dispersing factor (PDF)-expressing LNvs and subsets of dorsal lateral neurons (LNds) and dorsal neuron clusters (DN1 and DN2). To address the function of WAKE in LNv neurons, we examined the sleep phenotypes of flies with knockdown of WAKE in these cells. As shown in Figures 3D and 3E, the use of *Pdf-Gal4* and *cry-Gal4* (which drives expression in all LNvs and subsets of LNds and DNs) (Zhao et al., 2003) to drive *UAS-wake-miR1* caused significantly increased sleep latency and decreased sleep time, compared to both parental line controls. To ensure these phenotypes were not caused by "off-target" effects, we generated another *wake* microRNA line (*UAS-wake-miR2*) using different sequences from *CG42686* for the hairpin loops. As with the *UAS-wake-miR1* line, panneuronal expression of *UAS-wake-miR2* markedly reduced WAKE expression (Figure S2B). As expected, expression of *UAS-wake- miR2* using *wake-Gal4* or *Pdf-Gal4* also caused an increase in sleep latency compared to controls (Figure S3C).

Given that LNvs were previously shown to regulate sleep (Chung et al., 2009; Parisky et al., 2008; Shang et al., 2008; Sheeba et al., 2008), we next asked whether the loss of WAKE specifically in the LNvs accounts for the entire *wake* sleep phenotype. We used *Pdf-Gal80* (Stoleru et al., 2004) in combination with *wake-Gal4* to subtract the LNvs from WAKE+ cells (Figure 3F). Knockdown of WAKE in WAKE+ PDF– neurons did not result in a significant increase in sleep latency (Figure 3G) but did cause a decrease in sleep time

(Figure 3H). These data suggest that the wakefulness to sleep transition requires WAKE expression mainly in LNvs but that WAKE is also required in WAKE+ PDF– cells to regulate sleep maintenance, consistent with the idea that regulation of sleep initiation and sleep maintenance can be dissociated (Agosto et al., 2008).

Among the PDF+ LNvs, the large LNvs (l-LNvs) specifically have been shown to promote arousal (Chung et al., 2009; Parisky et al., 2008; Shang et al., 2008; Sheeba et al., 2008). Thus, we used *per-1b-Gal4* (which expresses in l-LNvs but not in small-LNvs) (Kaneko and Hall, 2000) and *R6-Gal4* (which expresses in small-LNvs but not l-LNvs) (Helfrich-Förster et al., 2007) to determine which subset of LNv cells requires WAKE function for proper timing of sleep onset. Expression of *UAS-wake-miR1* using *per-1b-Gal4*, but not *R6-Gal4*, caused a significant increase in sleep latency, suggesting that WAKE activity is specifically required in l-LNvs to regulate sleep onset (Figure 3I). Signaling from l-LNvs is thought to largely depend on PDF and its receptor PDFR, as these cells do not appear to express classical neurotransmitters (Taghert and Nitabach, 2012). Thus, we asked whether PDF/PDFR signaling is required for the effects of WAKE on sleep latency. We generated double mutants of *wake$^{D2}$* with *Pdf$^{01}$* or *Pdfr$^{han}$* (Hyun et al., 2005; Renn et al., 1999) and found that loss of PDF or its receptor essentially blocked the increase in sleep latency seen in *wake* mutants (Figure 3J).

## WIDE AWAKE Acts Downstream of CLK to Regulate Timing of Sleep Onset

Sleep is thought to be regulated by circadian and homeostatic processes (Borbély and Achermann, 1999). Because WAKE is expressed in clock neurons and is required for proper timing of sleep onset at the day/night transition, we hypothesized that WAKE acts to mediate the circadian timing of sleep onset. To address how the circadian clock regulates the timing of sleep, we examined sleep behavior in the canonical core clock mutants: *per*, *tim*, *Clk*, and *cyc* (Figure S4). Consistent with a previous report (Hendricks et al., 2003), we found that *Clk$^{jrk}$* and *cyc$^{01}$* mutants exhibited significantly reduced sleep, when compared to either controls or *per$^{01}$* and *tim$^{01}$* mutants (Figure S4A). In all four mutants, sleep bout duration was significantly reduced, compared to controls, suggesting that an intact circadian clock is important for sleep maintenance (Figure S4C).

To determine whether sleep initiation at the day/night transition was impaired in these clock mutants, we examined sleep latency in these flies. Interestingly, *Clk$^{jrk}$* and *cyc$^{01}$* mutants exhibited a marked increase in sleep latency, similar to *wake* flies. In contrast, *per$^{01}$* and *tim$^{01}$* flies showed the opposite phenotype, i.e., reduced sleep latency (Figures 4A and 4B). Along these lines, despite having markedly reduced sleep, *Clk$^{jrk}$* flies did not display a compensatory increase in sleep bout number (Figure S4D), consistent with a defect in sleep initiation. Because CLK and CYC are transcriptional activators, while PER and TIM act to inhibit the activity of CLK/CYC (Allada and Chung, 2010), these data suggest that molecules under CLK/CYC control regulate the timing of sleep onset at the sleep/wake transition.

We next assessed whether WAKE expression varies throughout the day. Indeed, WAKE levels cycle (Figures 4C and 4D), rising during the day and peaking in the early night around the time of sleep onset following lights off. To determine whether this daily variation of WAKE is dependent on CLK activity, we examined WAKE expression at the nadir (zeitgeber time 2 [ZT2]) and peak (ZT14) in control and *Clk$^{jrk}$* mutant backgrounds. As shown in Figures 4E and 4F, the increase in WAKE expression at ZT14 was absent in *Clk$^{jrk}$* flies, suggesting that cycling of WAKE expression is CLK dependent. Because WAKE acts in l-LNvs to regulate sleep onset (Figure 3), we next asked whether WAKE levels vary throughout the day specifically in these cells. We examined the transcriptional activity of *wake-Gal4* in l-LNvs during two time windows, using the photoconvertible fluorescent

protein KAEDE (Chen et al., 2012). Preexisting green KAEDE in the l-LNvs was converted into red KAEDE in living *wake-Gal4>UAS-kaede* flies by exposure to UV irradiation at ZT0 or ZT10 (Figure 4G). Ten hours after photoconversion, newly synthesized green KAEDE was ~3-fold higher during the night, compared to the day (Figures 4G and 4H). These data suggest that *wake* transcript cycles in the l-LNvs. Finally, we also assessed whether transcription of *wake* is CLK dependent specifically in l-LNvs. Indeed, in the $Clk^{jrk}$ background, *wake-Gal4* activity was dramatically reduced in l-LNvs but not in other nonclock neurons (Figures 4I and 4J). Taken together, these data strongly suggest that *wake* transcript cycles throughout the day specifically in l-LNvs and that CLK is required for expression of WAKE in these cells.

Given that proper timing of sleep onset depends on WAKE expression in LNvs, if WAKE acts downstream of CLK and CYC to regulate timing of sleep, we would expect that loss of CLK or CYC function in LNvs would also cause an increase in sleep latency. Indeed, flies that express dominant-negative forms of CLK or CYC specifically in the LNvs displayed a significant increase in sleep latency, compared to control flies (Figure 4K). We next asked whether restoration of WAKE in the LNvs in $Clk^{jrk}$ mutant flies could rescue their defects in sleep initiation at lights off. Importantly, we found that expression of WAKE specifically in LNvs had no effect on sleep latency in a wild-type background but rescued the increased sleep latency phenotype seen in $Clk^{jrk}$ flies (Figure 4L and Figure S4G). Similarly, WAKE expression in PDF+ cells rescued the increased sleep latency of $cyc^{01}$ flies (Figure S4E), but not that of *sleepless* (*sss*) flies (Figure S4F), supporting a specific role for WAKE downstream of CLK/CYC. The rescue of $Clk^{jrk}$ mutants by WAKE appears to be confined to the sleep latency phenotype, as other *Clk* phenotypes such as the arrhythmicity in DD conditions persisted when WAKE was expressed in PDF+ cells (Table S1). Taken together, these data strongly suggest that WAKE acts downstream of CLK/CYC to specifically promote sleep onset in the early night.

Our finding that *wake* mutants have normal circadian rhythms suggests that loss of WAKE impacts a circadian output pathway for sleep, rather than the phase or period of the core circadian oscillator. To confirm that the effects of WAKE on sleep latency are not secondary to effects on the core clock, we performed a series of experiments either knocking down WAKE or manipulating PDF+ neuron activity in the $per^{01}$ mutant background. Knockdown of WAKE by expressing *UAS-wake-miR1* in PDF+ cells or by the use of $wake^{D2}$ resulted in an increase in sleep latency that persisted in the $per^{01}$ mutant background (Figures S3D and S4H). Similarly, activation and inactivation of PDF+ cells using dTrpA1 or dORKΔC, respectively, also caused an increase and decrease of sleep latency in the $per^{01}$ mutant background (Figures S4I and S4J). Finally, we also examined whether loss of WAKE function or manipulation of PDF+ neuron activity affected circadian period length under DD conditions. Knockdown of WAKE in PDF+ cells using either *wake* microRNA line had no significant effect on period length, nor did activation or inactivation of PDF+ neurons (Table S1). Although reduction of CLK function in PDF+ cells did significantly increase period length in a minority of flies that were still rhythmic, similar effects were not observed with reduction of CYC function, and thus it is unlikely that the marked increase in sleep latency resulting from inhibition of CLK/CYC activity is due to lengthened period (Table S1). Together, these data demonstrate that WAKE acts downstream of the core circadian clock and that its effects on sleep latency are separable from the activity of the molecular oscillator.

## WIDE AWAKE Interacts with RDL and Upregulates Its Levels

Our data suggest that WAKE acts to convey circadian timing information to sleep/wake circuits to promote sleep. However, what is the molecular function of WAKE? Analysis of

the WAKE primary sequence reveals the presence of multiple potential protein-protein interaction domains. In addition, because WAKE is expressed in arousal-promoting cells but promotes sleep, we hypothesized that WAKE normally functions to inhibit the neurons in which it is expressed. Recent studies have shown that GABA signaling can inhibit LNvs through the GABA$_A$ receptor *Resistant to dieldrin* (RDL) to regulate sleep (Agosto et al., 2008; Chung et al., 2009; Parisky et al., 2008). Because *wake* mutants also exhibited increased sleep latency and decreased sleep time and because WAKE was expressed in LNvs, we sought to determine whether WAKE regulates RDL to modulate sleep. First, we examined whether *wake* and *Rdl* genetically interact, using *wake$^{D1}$* and a null allele of *Rdl* (*Rdl$^1$*). The sleep latency of *wake$^{D1}$/+* or *Rdl$^1$/+* heterozygous flies was similar to that of controls (Figure 5A). However, *wake$^{D1}$/Rdl$^1$* transheterozygous flies demonstrated a significant increase in sleep latency (Figure 5A), indicating that *wake$^{D1}$* and *Rdl$^1$* exhibit a dominant (transheterozygous) genetic interaction. Moreover, other *wake* alleles (*wake$^{D2}$* and *wake$^{P1}$*) also showed similar dominant genetic interactions with *Rdl$^1$* in sleep latency assays, as did two deficiencies of the *Rdl* locus—*Rdl$^{Df1}$* (*Df(3L)ED4416*) and *Rdl$^{Df2}$* (*Df(3L)BSC170*)—with *wake$^{D1}$* (Figure 5A and Figure S5A). These data demonstrate that this dominant interaction is not attributable to genetic background. This dominant genetic interaction between *wake* and *Rdl* was also observed in male flies, persisted in a *per$^{01}$* mutant background (Figure S5B), and did not alter circadian period length (Table S1). Finally, neither *Rdl* nor *wake* exhibited a dominant genetic interaction with other short-sleeping mutants, *sss* and *fmn* (Figure 5A), demonstrating the specificity of the interaction between *wake* and *Rdl*. Dominant genetic interactions are unusual and strongly suggest that WAKE and RDL act in the same pathway.

To address whether WAKE and RDL physically interact in a complex, we performed coimmunoprecipitation experiments. We removed the unstructured N-terminal domain of WAKE, as this domain rendered WAKE susceptible to degradation. We expressed this truncated WAKE (WAKE-T) alone, RDL alone, or both WAKE-T and RDL in *Xenopus* oocytes. We found that WAKE-T coimmunoprecipitated with RDL from *Xenopus* oocyte extracts (Figure 5B), suggesting that WAKE and RDL may physically interact in a complex. In contrast, as shown in Figure S5C, WAKE-T did not coimmunoprecipitate with a different receptor, the *Drosophila* adenosine receptor (dADOR) (Wu et al., 2009).

Next, we examined whether WAKE coexpression with RDL affects RDL levels in cultured *Drosophila* S2R+ cells. When RDL was coexpressed with WAKE, RDL protein levels increased approximately 2-fold (Figures 5C and 5D). In contrast, when WAKE was coexpressed with dADOR, there was no change in the levels of dADOR expression, suggesting that this effect is specific to RDL (Figures 5C and 5D). Together, these data demonstrate that *wake* and *Rdl* interact genetically and suggest that WAKE may form a complex with RDL to upregulate its expression.

Finally, we asked whether loss of WAKE would reduce RDL levels in vivo. To address this, we generated *UAS-RDL-myc* flies and used *Pdf-Gal4* to drive expression of RDL-myc in a *wake* mutant background. As shown in Figure 5E, RDL-myc expression was lower in the l-LNvs of *wake$^{D2}$* flies, compared to control flies. In particular, RDL-myc levels in the plasma membrane were significantly reduced in *wake* mutants versus control flies (Figure 5F). In contrast, there was no significant difference in perinuclear levels of RDL-myc between *wake* mutants and controls (Figure 5F). To rule out the possibility that WAKE affects *Pdf-Gal4* transcriptional activity in l-LNvs, we used *UAS-CD8::GFP* as a reporter to examine *Pdf-Gal4* transcription activity in these cells in the *wake* mutant background. As shown in Figures S5D and S5E, the CD8::GFP expression in the l-LNvs of *wake$^{D2}$* flies was similar to control flies, suggesting that loss of WAKE does not affect *Pdf-Gal4* activity. Together, these data suggest that not only is WAKE sufficient for upregulation of RDL

expression in cultured cells but that it is also necessary for proper RDL expression and plasma membrane targeting in l-LNv neurons.

## WAKE Reduces the Excitability of l-LNvs by Increasing GABA Sensitivity at Dusk

Our data suggest that WAKE acts in l-LNv neurons to upregulate RDL at the day/night transition, in order to promote sleep onset. If so, this should lead to relative silencing of these cells in the early night. It has previously been shown that both spontaneous action potential firing rate (AP rate) and resting membrane potential (RMP) cycle in l-LNvs, with a relative decrease in AP rate and hyperpolarization of the RMP at night (Cao and Nitabach, 2008). We thus investigated whether loss of WAKE would alter the excitability of l-LNv neurons in a time-dependent manner. We performed whole-cell current-clamp recordings of the l-LNv neurons in wild-type and *wake* mutant brains at ZT0–ZT2 and ZT12–ZT14. The AP rate was similar between *wake* and control l-LNvs at ZT0–ZT2 (Figures 6A and 6C). In contrast, the AP rate of the l-LNv cells in *wake* mutants was nearly 4-fold higher than controls at ZT12–ZT14, indicating that, in *wake* flies, these cells were more excitable specifically at the day/night transition (Figures 6A and 6C). As shown in Figure S6A, in control flies, the RMP of l-LNv cells was more hyperpolarized at ZT12–ZT14 compared to ZT0–ZT2 (although this difference was not significant). RMP of l-LNv cells in *wake* mutants was not significantly different between ZT0–ZT2 and ZT12–ZT14 (Figure S6A). A previous study showed that the AP rate of l-LNv cells is regulated by GABA signaling (McCarthy et al., 2011). Thus, we examined whether the reduction in AP rate at ZT12–ZT14 (versus ZT0– ZT2) was dependent on increased GABA signaling at that time. Indeed, using picrotoxin (PTX) to block $GABA_A$ receptors, the AP rate at ZT12–ZT14 was markedly increased and was similar to the AP rate at ZT0–ZT2 (Figure S6B). These data suggest that the excitability of l-LNvs is increased in *wake* mutants at dusk and that fast GABAergic signaling normally inhibits l-LNv excitability at that time.

Our data suggest that RDL levels are increased in a WAKE-dependent manner at dusk in l-LNvs. Thus, in *wake* mutants, RDL levels and the resulting sensitivity to GABA should be reduced in the early night. To examine this, we performed whole-cell voltage-clamp recordings on l-LNv neurons in wild-type and *wake* mutant backgrounds. It has previously been shown that GABA-evoked currents in l-LNvs can be blocked with application of PTX, suggesting that these currents mainly depend on $GABA_A$ receptors (Chung et al., 2009). To isolate the effects of GABA to the l-LNv cells, we used tetrodotoxin (TTX) to block AP firing in our preparation. As shown in Figures 6D and 6E, GABA-evoked currents at ZT11–ZT14 were significantly reduced in *wake* mutants, demonstrating that the l-LNvs in these mutants exhibit reduced GABA sensitivity at dusk. Thus, our electrophysiological data support our model (Figure 6F; Discussion) that the function of WAKE is to promote sleep onset by increasing GABA sensitivity and inhibiting the excitability of l-LNvs at the day/night transition.

Interestingly, previous studies have shown that the molecular clock in l-LNvs does not cycle in DD (Shafer et al., 2002; Yang and Sehgal, 2001) and that, under these conditions, PER remains in the nucleus in these cells (Shafer et al., 2002). We thus wondered how WAKE expression and function would be affected in DD. Because PER can suppress CLK function and WAKE expression is CLK dependent, we hypothesized that *wake* transcription would be reduced in DD compared to light: dark (LD). Indeed, in the l-LNvs, newly synthesized green KAEDE driven by *wake-Gal4* was decreased ~2-fold in DD versus LD (Figures S6C and S6D). This decrease of WAKE in DD would be predicted to enhance the excitability of the l-LNvs in DD versus LD. As shown in Figure S6E, whole-cell patch-clamp recordings of l-LNvs demonstrated that the AP rate of l-LNvs was significantly increased in circadian time 12–14 (CT12– CT14) compared to ZT12–ZT14 (Figure S6E). Moreover, when we restored

WAKE levels in DD by overexpressing WAKE in l-LNvs, sleep latency at CT12 was significantly reduced, similar to that seen in ZT12 (Figure S6F), and sleep time was also increased (Figure S6G). Given that the core oscillator in the l-LNvs does not cycle in DD, it is intriguing that the sleep phenotypes of *wake* mutants persist in DD (Figures 1G and 1H). Our data (Figures S6C–S6E) suggest that, with respect to WAKE levels, wild-type flies under DD conditions are analogous to *wake* partial loss-of function mutants. Since our *wake* mutants are null alleles, we expect the AP firing rate of l-LNvs in DD to be increased in *wake* mutants, compared to controls. Indeed, at CT12, l-LNv AP rate is higher in *wake* mutants than in controls (Figure S6E). Thus, both in LD and DD, WAKE reduces the AP firing rate in l-LNvs and consequently promotes sleep onset. Finally, our data also suggest the reduced sleep and increased sleep latency seen in wild-type flies in DD relative to LD is mediated, at least in part, by a reduction of WAKE levels.

### The Mouse Homolog of WIDE AWAKE Is Expressed in the SCN

We identified a single homolog of WAKE (ANKFN1) in mice, using BLAST (33% identity and 56% similarity over 537 amino acids containing the ankryin repeats and fibronectin domain) (Figure 7A). As a first step in evaluating the potential function of this putative homolog of WAKE, we performed in situ hybridization of functionally wild-type adult male *Lhx1$^{lox/lox}$* mouse brains with two different probes. Both probes revealed similar expression patterns, and the data from one of the probes are shown in Figures 7B and 7C. Strikingly, *ANKFN1* transcript was enriched in the SCN, the master circadian pacemaker in mammals (Figure 7B). We compared colocalization of *ANKFN1* with neuropeptide markers that label distinct SCN subdomains, including gastrin-releasing peptide (*GRP*), vasoactive intestinal polypeptide (*VIP*), and arginine vasopressin (*AVP*). *ANKFN1* expression largely overlaps the *GRP*-expressing domain, suggesting it is specifically expressed in the core region of the SCN (Figure 7C). The Allen Brain Atlas (http://www.brain-map.org) also demonstrates SCN enrichment of *ANKFN1* in a pattern similar to our data. This expression pattern is reminiscent of the expression of WAKE in flies, since PDF+ neurons also contain circadian pacemaker cells and because the l-LNv cells receive light input, similar to the SCN core. These findings suggest that the function of WAKE is conserved in mammals.

## DISCUSSION

The molecular pathways by which the circadian clock modulates the timing of sleep are unknown. Here, we identify a molecule, WIDE AWAKE, that promotes sleep and is required for circadian timing of sleep onset. Our data argue for a direct role for the circadian oscillator in regulating sleep and support a model whereby WAKE acts as a molecular intermediary between the circadian clock and sleep. In this model, WAKE transmits timing information from the circadian clock to inhibit arousal circuits at dusk, thus facilitating the transition from wake to sleep (Figure 6F). *wake* is transcriptionally upregulated by CLK activity, specifically in LNv clock neurons. WAKE levels in l-LNvs rise during the day and peak at the early night, near the wake/sleep transition. This increase in WAKE levels upregulates RDL in l-LNvs, enhancing their sensitivity to GABA signaling and serving to inhibit the l-LNv arousal circuit. In this manner, cycling of WAKE promotes cycling of the excitability of l-LNv cells. In *wake* mutants, l-LNvs lose this circadian electrical cycling; the higher firing rate of these cells at dusk leads to increased release of PDF, which would act on PDFR on downstream neurons to inhibit sleep onset. The identity of the GABAergic neurons signaling to the l-LNvs is currently unknown, but if they serve to convey information about sleep pressure from homeostatic circuits, the l-LNvs could serve as a site of integration for homeostatic and circadian sleep regulatory signals (Figure 6F).

Although WAKE is expressed in clock neurons and its levels vary throughout the day, WAKE itself is not a core clock molecule, since period length and activity rhythm strength are intact in *wake* mutants in constant darkness. We also show that the effects of WAKE on sleep latency are not attributable to alterations in core clock function. In addition, because locomotor rhythm strength is intact in *wake* mutants, WAKE is not a clock output molecule for locomotor rhythms. Rather, WAKE is, to our knowledge, the first clock output molecule shown to specifically regulate sleep timing.

Previous studies have demonstrated that RDL in LNvs regulates sleep in *Drosophila* (Chung et al., 2009; Parisky et al., 2008). Our work further implicates RDL as a key factor in the circadian modulation of sleep. In mammals, the localization and function of GABA$_A$ receptors are regulated by a variety of cytosolic accessory proteins, some of which are associated with the plasma membrane and cytoskeletal elements (Luscher et al., 2011). Our data suggest that WAKE acts as an accessory protein for RDL, upregulating its levels and promoting its targeting to the plasma membrane. RDL is broadly expressed throughout the adult *Drosophila* brain (Harrison et al., 1996), whereas WAKE appears more spatially restricted. It is likely that RDL is regulated by WAKE in specific cells (e.g., WAKE+ cells), while in other cells that express RDL but not WAKE, other factors are involved. Together, these data suggest a model in which increased GABA sensitivity is required in specific arousal circuits to facilitate rapid and complete switching between sleep/wake states at the appropriate circadian time.

Intriguingly, our data, as well as data from the Allen Brain Atlas, suggest that the putative mouse homolog of WAKE (*ANKFN1*) is enriched in the mouse SCN, the master circadian pacemaker in mammals. Specifically, ANKFN1 is expressed in the "core" region of the SCN, which is analogous to the large LNvs in flies, in that it receives light input and its molecular oscillator does not cycle or cycles weakly in DD (Yan et al., 2007). These observations support a potential conservation of WAKE function in regulating clock-dependent timing of sleep onset, which will be evaluated by our ongoing genetic analysis in mice. The pronounced difficulty of *wake* flies to fall asleep at lights off is reminiscent of sleep-onset insomnia in humans. Moreover, the most widely used medications for the treatment of insomnia are GABA agonists (Nutt and Stahl, 2010). Thus, the identification of a molecule that mediates circadian timing of sleep onset by promoting GABA signaling may lead to a deeper understanding of mechanisms underlying insomnia and its potential therapies.

## EXPERIMENTAL PROCEDURES

### Sleep and Circadian Assays

Sleep assays were generally performed as previously described (Liu et al., 2012). For sleep measurements, 4- to 7-day-old flies were monitored at 25°C in glass tubes containing 5% sucrose and 2% agar using the *Drosophila* Activity Monitoring System (Trikinetics). Female flies were used unless otherwise stated. Activity counts were collected in 1 min bins in LD for 2 days, and a moving window was used to identify sleep as periods of inactivity lasting at least 5 min (Shaw et al., 2000). Sleep parameters were computed using MATLAB-based (MathWorks) custom software. For analysis of sleep in constant darkness (DD), the first day in DD was analyzed, CT12 was determined using the period lengths of individual flies, and sleep latency was then calculated from CT12. For *UAS-dTrpA1* experiments, flies were raised at 22°C, 1 day of data was recorded at 22°C as a baseline day, and 1 day was recorded at 29°C, in order to activate the relevant neurons. For *elav-Geneswitch* experiments, either 250 μM RU486 dissolved in ethanol or ethanol alone was added to 5% sucrose/2% agar food. For analysis of circadian behavior, activity counts were collected in 30 min bins in DD over a 6-day period and analyzed using ClockLab (Actimetrics). Period length (tau) was

determined by $\chi^2$ periodogram analysis, and rhythm strength was measured by relative FFT, calculated by fast Fourier transform analysis.

## Immunostaining

Immunostaining of whole-mount brain samples was performed essentially as follows: brains were fixed in 4% PFA for 1 hr; after washing, samples were incubated with mouse anti-GFP (Clontech) at 1:1,000, rabbit anti-GFP (Invitrogen) at 1:1,000, rabbit anti-PER (Stanewsky et al., 1997) at 1:8,000, rat anti-PER at 1:1,500, mouse anti-MYC (9E10, Developmental Studies Hybridoma Bank [DSHB]) at 1:500, mouse anti-PDF (DSHB) at 1:400, or mouse nc82 (DSHB) at 1:100 at 4°C overnight; after additional washes, samples were incubated with Alexa 488 anti-mouse (Invitrogen, 1:2,000), Alexa 488 anti-rabbit (Invitrogen, 1:2,000), Alexa 568 anti-rabbit (Invitrogen, 1:2,000), Alexa 568 anti-mouse (Invitrogen, 1:1,000), Cy5 anti-mouse (Rockland, 1:1,000), Alexa 647 anti-rabbit (Invitrogen, 1:5,000), Cy5 anti-Rat (Rockland, 1:1,000) overnight at 4°C. Images were obtained on a Leica TCS-SP5 or Zeiss LSM700 with 1-μm-thick sections under 20×, 25×, 60×, or 63× magnification. For anti-MYC stainings, Alexa 568 anti-mouse (for anti-MYC) and Cy5 anti-Rat (for anti-PER) were used for secondary antibodies, and stainings were performed at ~ZT0. Images were taken under 63× magnification and acquired as $1,024 \times 1,024$ pixels. ImageJ software was used for quantification; intensity of total, plasma membrane, and perinuclear (likely consisting of endoplasmic reticulum) signal was calculated. For total signal intensity, the sum of all pixel intensities of a stack comprising the whole cell was calculated. For plasma membrane versus perinuclear signal, the 1 μm slice with the strongest nuclear PER signal was used to quantify the appropriate region of interest (ROI) from each cell. To measure plasma membrane signal, the following was performed: first, an ROI was drawn around the entire cell, and the total intensity was measured (ROI1); second, within this slice, another ROI was drawn starting from 4–6 pixels (~500 nm) inside ROI1, containing the cytoplasmic, perinuclear, and nuclear regions, and its intensity was measured (ROI2); and, third, intensity of plasma membrane signal was calculated as $I_{ROI1} - I_{ROI2}$. To measure perinuclear signal, in the same slice, we drew ROIs around the perinuclear region (ROI3) and nuclear region (ROI4), and we calculated perinuclear intensity as $I_{ROI3} - I_{ROI4}$.

## KAEDE Measurement

The diurnal synthesis of KAEDE protein in l-LNvs of *wake-Gal4>UAS-kaede* flies was measured as previously described (Chen et al., 2012). A single fly restricted in a pipette tip was UV irradiated for 5 min through an objective lens (maximum intensity, working distance ~1 mm). Photoconverted flies were separated into two groups. Fluorescence was measured immediately for one group and 10 hr later for the other group. All brains were directly imaged using LSM700 without fixation. Green and red KAEDE were excited by 488 nm and 543 nm lasers, respectively. l-LNv neurons were located in less than 10 s by fast prescanning of red KAEDE (543 nm). A single optical slice through the cell bodies was taken under a 63× water-immersion objective lens. Using ImageJ, the rate of green KAEDE synthesis was calculated with the formula $(F_{t1} - F_{t0})/F_{t0}$, where $F_{t0}$ and $F_{t1}$ are the ratio of intensities between green and red signal immediately after photoconversion (t0) and 10 hr later (t1), respectively.

## Whole-Cell Patch-Clamp Recordings

Four- to six-day-old *Pdf-Gal4 > UAS-CD8::GFP* female flies from WT and *wake^{D2}* backgrounds were used, after entrainment to a 12 hr:12 hr LD cycle for at least 3 days. Brains were removed in a *Drosophila* physiological saline solution (101 mM NaCl, 3 mM KCl, 1 mM $CaCl_2$, 4 mM $MgCl_2$, 1.25 mM $NaH_2PO_4$, 20.7 mM $NaHCO_3$, and 5 mM glucose [pH 7.2]), which was prebubbled with 95% $O_2$ and 5% $CO_2$. Brains were then

treated with 2 mg/ml protease XIV (Sigma-Aldrich) for 5–8 min at 22°C. l-LNvs were visualized by GFP fluorescence or infrared-differential interference contrast (IR-DIC) optics using a fixed-stage upright microscope (BX51WI; Olympus). To minimize the effect of light in the "dusk" experiments, light level was kept at 2–20 lux.

Whole-cell recordings were performed at room temperature. Patch-pipettes (5–9 M$\Omega$) were fashioned from borosilicate glass capillary with a Flaming- Brown puller (P-1000; Sutter Instrument). The internal solution used for current- clamp recording contained 102 mM potassium gluconate, 0.085 mM $CaCl_2$, 0.94 mM EGTA, 8.5 mM HEPES, 4 mM Mg-ATP, 0.5 mM Na-GTP, and 17 mM NaCl (pH 7.2). Potassium in the patch-pipette was replaced with cesium for voltage-clamp recordings. To label recorded cells, we included 13 mM biocytin hydrazide in the pipette solution. Cells were rejected if $R_{access} > 50$ M$\Omega$. Recordings were acquired with an Axopatch 200B amplifier (Molecular Devices) and Digidata 1440A interface (Molecular Devices). Signals were sampled at 20 kHz and low-pass filtered at 2 kHz in current-clamp recording or at 100 Hz in voltage-clamp recording.

In order to confirm the identity of the recorded cell, brains were immunostained after the recording essentially as described above, using mouse anti-GFP (Invitrogen, 1:200) for 16–40 hr at 4°C, followed by incubation with Alexa 488 anti-mouse (Invitrogen, 1:1,000) and Alexa-568-conjugated streptavidin (Invitrogen, 1:100) for 24–40 hr at 4°C. Only samples in which a single cell was both dye labeled and GFP positive were included in the analyses.

### Statistical Analysis

For comparisons of two groups of normally distributed data, t tests were performed. For multiple comparisons, one-way ANOVAs followed by post hoc Tukey were performed. For multiple comparisons of nonnormally distributed data, Kruskal-Wallis tests were performed, with Bonferroni correction for post hoc comparisons. Log rank tests were used to compare longevity of experimental and control animals.

## Supplementary Material

Refer to Web version on PubMed Central for supplementary material.

## Acknowledgments

## References

Agosto J, Choi JC, Parisky KM, Stilwell G, Rosbash M, Griffith LC. Modulation of GABAA receptor desensitization uncouples sleep onset and maintenance in *Drosophila*. Nat Neurosci. 2008; 11:354–359. [PubMed: 18223647]

Allada R, Chung BY. Circadian organization of behavior and physiology in *Drosophila*. Annu Rev Physiol. 2010; 72:605–624. [PubMed: 20148690]

Borbély AA, Achermann P. Sleep homeostasis and models of sleep regulation. J Biol Rhythms. 1999; 14:557–568. [PubMed: 10643753]

Cao G, Nitabach MN. Circadian control of membrane excitability in *Drosophila melanogaster* lateral ventral clock neurons. J Neurosci. 2008; 28:6493–6501. [PubMed: 18562620]

Chen CH, Huang H, Ward CM, Su JT, Schaeffer LV, Guo M, Hay BA. A synthetic maternal-effect selfish genetic element drives population replacement in *Drosophila*. Science. 2007; 316:597–600. [PubMed: 17395794]

Chen CC, Wu JK, Lin HW, Pai TP, Fu TF, Wu CL, Tully T, Chiang AS. Visualizing long-term memory formation in two neurons of the *Drosophila* brain. Science. 2012; 335:678–685. [PubMed: 22323813]

Chung BY, Kilman VL, Keath JR, Pitman JL, Allada R. The GABA(A) receptor RDL acts in peptidergic PDF neurons to promote sleep in *Drosophila*. Curr Biol. 2009; 19:386–390. [PubMed: 19230663]

Cirelli C, Bushey D, Hill S, Huber R, Kreber R, Ganetzky B, Tononi G. Reduced sleep in *Drosophila* Shaker mutants. Nature. 2005; 434:1087–1092. [PubMed: 15858564]

Dyson HJ, Wright PE. Intrinsically unstructured proteins and their functions. Nat Rev Mol Cell Biol. 2005; 6:197–208. [PubMed: 15738986]

Eastman CI, Mistlberger RE, Rechtschaffen A. Suprachiasmatic nuclei lesions eliminate circadian temperature and sleep rhythms in the rat. Physiol Behav. 1984; 32:357–368. [PubMed: 6463124]

Harrison JB, Chen HH, Sattelle E, Barker PJ, Huskisson NS, Rauh JJ, Bai D, Sattelle DB. Immunocytochemical mapping of a C-terminus anti-peptide antibody to the GABA receptor subunit, RDL in the nervous system in *Drosophila melanogaster*. Cell Tissue Res. 1996; 284:269–278. [PubMed: 8625394]

Helfrich-Förster C, Shafer OT, Wülbeck C, Grieshaber E, Rieger D, Taghert P. Development and morphology of the clock-gene-expressing lateral neurons of *Drosophila melanogaster*. J Comp Neurol. 2007; 500:47–70. [PubMed: 17099895]

Hendricks JC, Finn SM, Panckeri KA, Chavkin J, Williams JA, Sehgal A, Pack AI. Rest in *Drosophila* is a sleep-like state. Neuron. 2000; 25:129–138. [PubMed: 10707978]

Hendricks JC, Lu S, Kume K, Yin JC, Yang Z, Sehgal A. Gender dimorphism in the role of cycle (BMAL1) in rest, rest regulation, and longevity in *Drosophila melanogaster*. J. Biol. Rhythms. 2003; 18:12–25.

Hyun S, Lee Y, Hong ST, Bang S, Paik D, Kang JK, Shin J, Lee J, Jeon K, Hwang S, et al. *Drosophila* GPCR Han is a receptor for the circadian clock neuropeptide PDF. Neuron. 2005; 48:267–278. [PubMed: 16242407]

Kaneko M, Hall JC. Neuroanatomy of cells expressing clock genes in *Drosophila*: transgenic manipulation of the period and timeless genes to mark the perikarya of circadian pacemaker neurons and their projections. J Comp Neurol. 2000; 422:66–94. [PubMed: 10842219]

Koh K, Joiner WJ, Wu MN, Yue Z, Smith CJ, Sehgal A. Identification of SLEEPLESS, a sleep-promoting factor. Science. 2008; 321:372–376. [PubMed: 18635795]

Liu Q, Liu S, Kodama L, Driscoll MR, Wu MN. Two dopaminergic neurons signal to the dorsal fan-shaped body to promote wakefulness in *Drosophila*. Curr Biol. 2012; 22:2114–2123. [PubMed: 23022067]

Lowrey PL, Takahashi JS. Genetics of circadian rhythms in Mammalian model organisms. Adv Genet. 2011; 74:175–230. [PubMed: 21924978]

Luscher B, Fuchs T, Kilpatrick CL. GABAA receptor trafficking mediated plasticity of inhibitory synapses. Neuron. 2011; 70:385–409. [PubMed: 21555068]

McCarthy EV, Wu Y, Decarvalho T, Brandt C, Cao G, Nitabach MN. Synchronized bilateral synaptic inputs to *Drosophila melanogaster* neuropeptidergic rest/arousal neurons. J Neurosci. 2011; 31:8181–8193. [PubMed: 21632940]

Mosavi LK, Cammett TJ, Desrosiers DC, Peng ZY. The ankyrin repeat as molecular architecture for protein recognition. Protein Sci. 2004; 13:1435–1448. [PubMed: 15152081]

Nutt DJ, Stahl SM. Searching for perfect sleep: the continuing evolution of GABAA receptor modulators as hypnotics. J Psychopharmacol (Oxford). 2010; 24:1601–1612. [PubMed: 19942638]

Osterwalder T, Yoon KS, White BH, Keshishian H. A conditional tissue-specific transgene expression system using inducible GAL4. Proc Natl Acad Sci USA. 2001; 98:12596–12601. [PubMed: 11675495]

Parisky KM, Agosto J, Pulver SR, Shang Y, Kuklin E, Hodge JJ, Kang K, Liu X, Garrity PA, Rosbash M, Griffith LC. PDF cells are a GABA-responsive wake-promoting component of the *Drosophila* sleep circuit. Neuron. 2008; 60:672–682. [PubMed: 19038223]

Parks AL, Cook KR, Belvin M, Dompe NA, Fawcett R, Huppert K, Tan LR, Winter CG, Bogart KP, Deal JE, et al. Systematic generation of high-resolution deletion coverage of the *Drosophila melanogaster* genome. Nat Genet. 2004; 36:288–292. [PubMed: 14981519]

Renn SCP, Park JH, Rosbash M, Hall JC, Taghert PH. A pdf neuropeptide gene mutation and ablation of PDF neurons each cause severe abnormalities of behavioral circadian rhythms in *Drosophila*. Cell. 1999; 99:791–802. [PubMed: 10619432]

Rogulja D, Young MW. Control of sleep by cyclin A and its regulator. Science. 2012; 335:1617–1621. [PubMed: 22461610]

Roy S, Ernst J, Kharchenko PV, Kheradpour P, Negre N, Eaton ML, Landolin JM, Bristow CA, Ma L, Lin MF, et al. Identification of functional elements and regulatory circuits by *Drosophila* modENCODE. Science. 2010; 330:1787–1797. [PubMed: 21177974]

Shafer OT, Rosbash M, Truman JW. Sequential nuclear accumulation of the clock proteins period and timeless in the pacemaker neurons of *Drosophila melanogaster*. J Neurosci. 2002; 22:5946–5954. [PubMed: 12122057]

Shang Y, Griffith LC, Rosbash M. Light-arousal and circadian photoreception circuits intersect at the large PDF cells of the *Drosophila* brain. Proc. Natl. Acad. Sci. USA. 2008; 105:19587–19594.

Shaw PJ, Cirelli C, Greenspan RJ, Tononi G. Correlates of sleep and waking in *Drosophila melanogaster*. Science. 2000; 287:1834–1837. [PubMed: 10710313]

Shaw PJ, Tononi G, Greenspan RJ, Robinson DF. Stress response genes protect against lethal effects of sleep deprivation in *Drosophila*. Nature. 2002; 417:287–291. [PubMed: 12015603]

Sheeba V, Fogle KJ, Kaneko M, Rashid S, Chou YT, Sharma VK, Holmes TC. Large ventral lateral neurons modulate arousal and sleep in *Drosophila*. Curr Biol. 2008; 18:1537–1545. [PubMed: 18771923]

Shiromani PJ, Xu M, Winston EM, Shiromani SN, Gerashchenko D, Weaver DR. Sleep rhythmicity and homeostasis in mice with targeted disruption of mPeriod genes. Am J Physiol Regul Integr Comp Physiol. 2004; 287:R47–R57. [PubMed: 15031135]

Stanewsky R, Frisch B, Brandes C, Hamblen-Coyle MJ, Rosbash M, Hall JC. Temporal and spatial expression patterns of transgenes containing increasing amounts of the *Drosophila* clock gene period and a lacZ reporter: mapping elements of the PER protein involved in circadian cycling. J Neurosci. 1997; 17:676–696. [PubMed: 8987790]

Stavropoulos N, Young MW. insomniac and Cullin-3 regulate sleep and wakefulness in *Drosophila*. Neuron. 2011; 72:964–976. [PubMed: 22196332]

Stoleru D, Peng Y, Agosto J, Rosbash M. Coupled oscillators control morning and evening locomotor behaviour of *Drosophila*. Nature. 2004; 431:862–868. [PubMed: 15483615]

Taghert PH, Nitabach MN. Peptide neuromodulation in invertebrate model systems. Neuron. 2012; 76:82–97. [PubMed: 23040808]

Toh KL, Jones CR, He Y, Eide EJ, Hinz WA, Virshup DM, Ptácek LJ, Fu YH. An hPer2 phosphorylation site mutation in familial advanced sleep phase syndrome. Science. 2001; 291:1040–1043. [PubMed: 11232563]

Wu MN, Koh K, Yue Z, Joiner WJ, Sehgal A. A genetic screen for sleep and circadian mutants reveals mechanisms underlying regulation of sleep in *Drosophila*. Sleep. 2008; 31:465–472. [PubMed: 18457233]

Wu MN, Ho K, Crocker A, Yue Z, Koh K, Sehgal A. The effects of caffeine on sleep in *Drosophila* require PKA activity, but not the adenosine receptor. J Neurosci. 2009; 29:11029–11037. [PubMed: 19726661]

Xu Y, Padiath QS, Shapiro RE, Jones CR, Wu SC, Saigoh N, Saigoh K, Ptácek LJ, Fu YH. Functional consequences of a CKIdelta mutation causing familial advanced sleep phase syndrome. Nature. 2005; 434:640–644. [PubMed: 15800623]

Yan L, Karatsoreos I, Lesauter J, Welsh DK, Kay S, Foley D, Silver R. Exploring spatiotemporal organization of SCN circuits. Cold Spring Harb Symp Quant Biol. 2007; 72:527–541. [PubMed: 18419312]

Yang Z, Sehgal A. Role of molecular oscillations in generating behavioral rhythms in *Drosophila*. Neuron. 2001; 29:453–467. [PubMed: 11239435]

Zhao J, Kilman VL, Keegan KP, Peng Y, Emery P, Rosbash M, Allada R. *Drosophila* clock can generate ectopic circadian clocks. Cell. 2003; 113:755–766. [PubMed: 12809606]
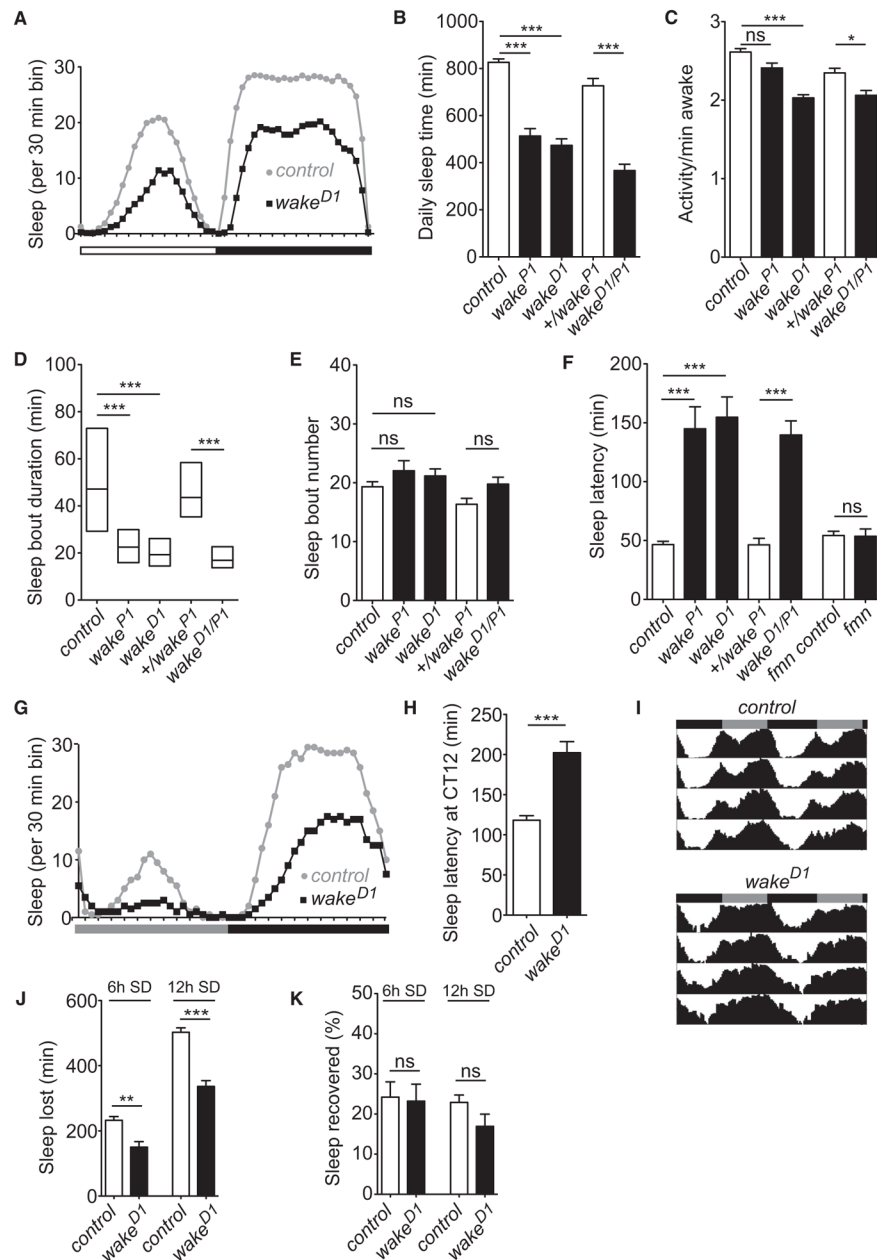
**Figure 1. Sleep Phenotypes of *wake* Mutants**

(A) Sleep profile of background control flies (gray circles) (n = 118) versus *wake$^{D1}$* flies (black squares) (n = 73), plotted in 30 min bins. White and black bars indicate 12 hr light and dark periods, respectively.

(B–F) Daily sleep time (B), waking activity (C), sleep bout duration (D), sleep bout number (E), and sleep latency (F) for control (n = 118), *wake$^{P1}$* (n = 41), *wake$^{D1}$* (n = 73), +/ *wake$^{P1}$* (n = 31), and *wake$^{D1}$/ wake$^{P1}$* (n = 31) flies. For (F), data for *fmn control* (n = 31) and *fmn* (n = 43) are also shown.

(G) Sleep profile in constant darkness (DD) of control flies (gray circles) (n = 53) versus *wake$^{D1}$* flies (black squares) (n = 65). Gray and black bars indicate 12 hr subjective day and night, respectively.

(H and I) Sleep latency at subjective night (H) and average activity records (I) in DD of control versus *wake^{D1}* flies. The activity records are double plotted so that each horizontal line represents data for 2 days.

(J and K) Sleep lost (J) and percentage of sleep recovered (K) for flies undergoing sleep deprivation for 6 hr (control, n = 48; *wake^{D1}*, n = 32) or 12 hr (control, n = 54; *wake^{D1}*, n = 30). Mean ± SEM is shown. "*," "**," "***," and "ns" denote p < 0.05, p < 0.01, p < 0.001, and not significant, respectively. Sleep bout duration, which is not normally distributed, is shown as simplified box plots, where the line inside the box indicates the median, and the top and bottom represent 75% and 25%, respectively. See also Figure S1.
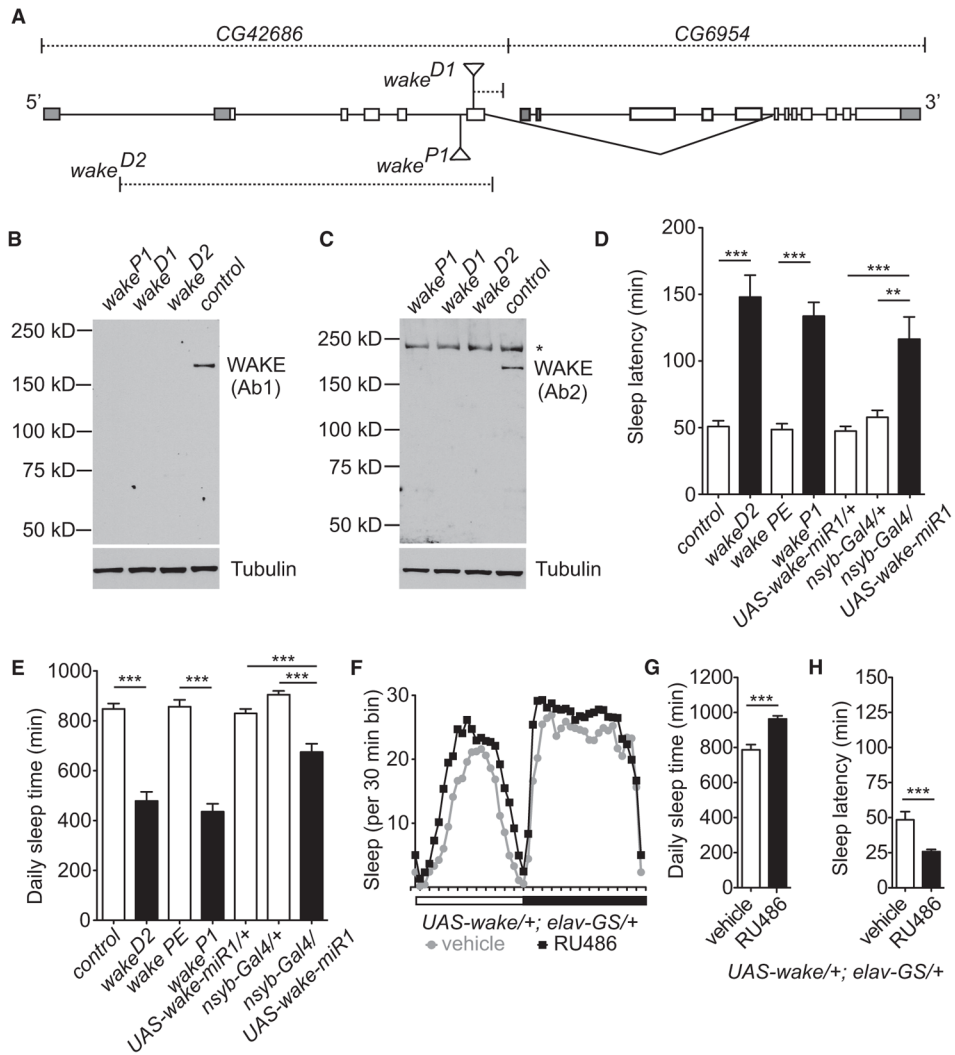
**Figure 2. Molecular Cloning and Genetic Analysis of *wake***

(A) Schematic of the genomic region of *wake-FL*, which includes sequence from *CG42686* and *CG6954*. White boxes and gray boxes indicate coding and noncoding exons, respectively. Deletions in *wake^D1^* and *wake^D2^* are shown as dashed lines. The splicing event between *CG42686* and *CG6954* is indicated by the caret symbol.

(B and C) Western blot analysis of control, *wake^P1^*, *wake^D1^*, and *wake^D2^* head extracts by WAKE-Ab1 (B) and WAKE-Ab2 (C). In (C), "*" indicates nonspecific bands detected in all samples. In this and subsequent western blots, Tubulin was used as a loading control.

(D and E) Sleep latency (D) and daily sleep time (E) of background control (control, n = 38), *wake^D2^* (n = 40), precise excision of *wake^P1^* (*wake PE*, n = 33), *wake^P1^* (n = 40), *UAS-wake-miR1/+* (n = 63), *nsyb-Gal4/+* (n = 34), and *nsyb-Gal4/UAS-wake-miR1* (n = 31) flies.

(F) Sleep profile of vehicle-fed (gray circles) (n = 26) versus 250 μM RU486-fed (black squares) (n = 28) *UAS-wake/+; elav-Geneswitch (elav-GS)/+* flies, plotted in 30 min bins. White and black bars indicate 12 hr light and dark periods, respectively.

(G and H) Daily sleep time (G) and sleep latency (H) of flies in (F). Mean ± SEM is shown. See also Figure S2.
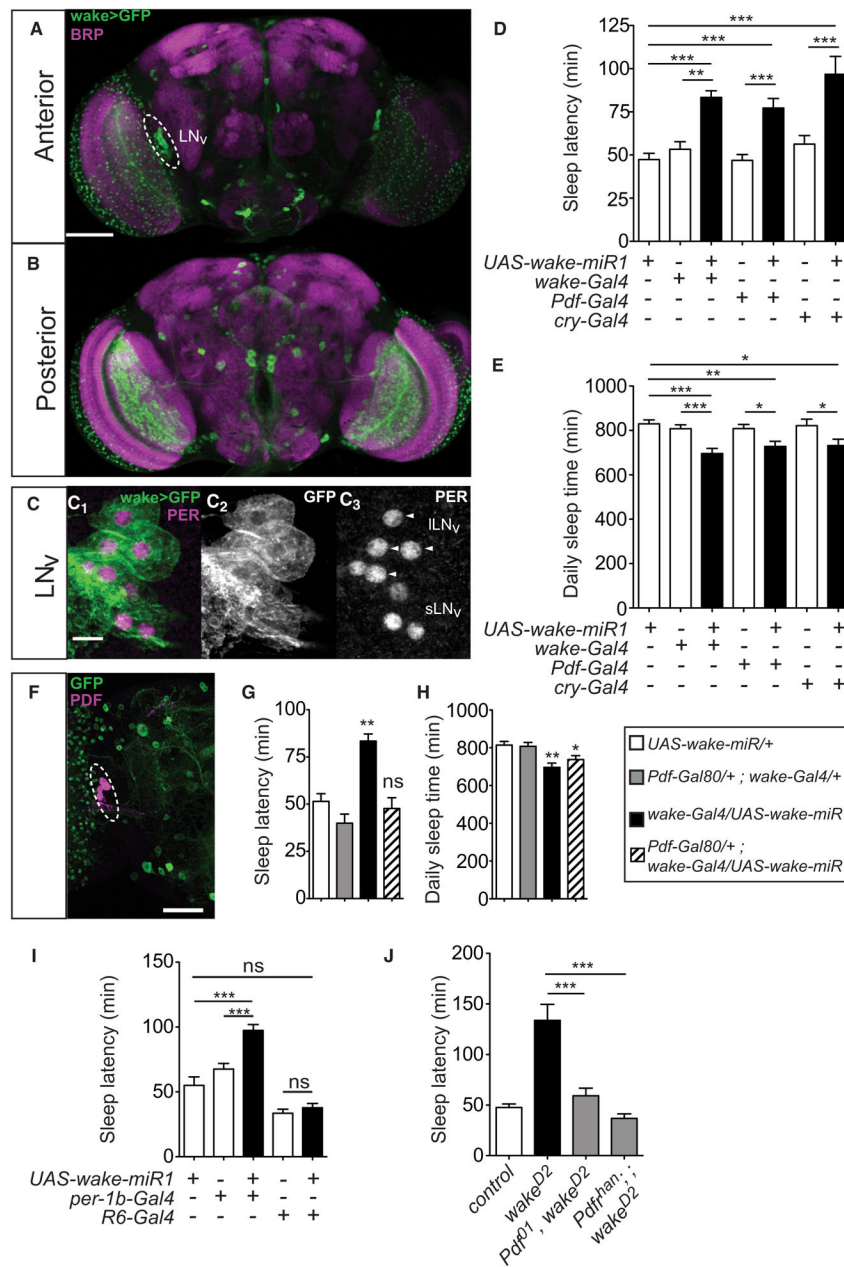
**Figure 3. WAKE Is Expressed in a Subset of Neurons in the Adult Brain, Including Clock Neurons that Promote Arousal**

(A and B) Whole-mount brain immunostaining of *wake-Gal4 > UAS-CD8::GFP* flies with anti-GFP (green) and anti-Bruchpilot (BRP, nc82, magenta). Maximal intensity projection of 1 μm confocal sections of the anterior half (A) and posterior half (B) of an adult brain. The dashed ellipse outlines the LNv cells.

(C) Anti-GFP (green) and anti-PER (magenta) immunostaining of LNvs in a *wake-Gal4 > UAS-CD8::GFP* fly brain. Merged (C₁), anti-GFP (C₂), anti-PER (C₃) panels are shown. Arrowheads in (C₃) indicate l-LNv cells.

(D and E) Sleep latency (D) and daily sleep time (E) of *UAS-wake-miR1*/+ (n = 63), *wake-Gal4*/+ (n = 45), *wake-Gal4/UAS-wake-miR1* (n = 41), *Pdf-Gal4*/+ (n = 75), *Pdf-Gal4*/+;

*UAS-wake-miR1*/+ (n = 57), *cry-Gal4-16*/+ (n = 39), and *cry-Gal4-16*/*UAS-wake-miR1* (n = 36) flies.

(F) Whole-mount brain immunostaining of *Pdf-Gal80/UAS-CD8::GFP; wake-Gal4/+* flies with anti-GFP (green) and anti-PDF (magenta). Maximal intensity projection of the entire brain is shown. The dashed ellipse outlines the location of the LNv cells.

(G and H) Sleep latency (G) and daily sleep time (H) of *UAS-wake-miR1/+* (n = 50), *Pdf-Gal80/+; wake-Gal4/+* (n = 49), *wake-Gal4/UAS-wake-miR1* (n = 26), and *Pdf-Gal80/+; wake-Gal4/UAS-wake-miR1* (n = 47) flies.

(I) Sleep latency of *UAS-wake-miR1/+* (n = 34), *per-1b-Gal4/+* (n = 47), *per-1b-Gal4/+; UAS-wake-miR1/+* (n = 52), *R6-Gal4/+* (n = 26), and *R6-Gal4/+; UAS-wake-miR1/+* (n = 33) flies.

(J) Sleep latency of background control (n = 62), *wake$^{D2}$* (n = 39), *Pdf$^{01}$,wake$^{D2}$* (n = 37), and *Pdfr$^{han}$; ; wake$^{D2}$* (n = 27) flies. Scale bar denotes 100 μm in (A) and (F) and 10 μm in (C). Mean ± SEM is shown. See also Figure S3.
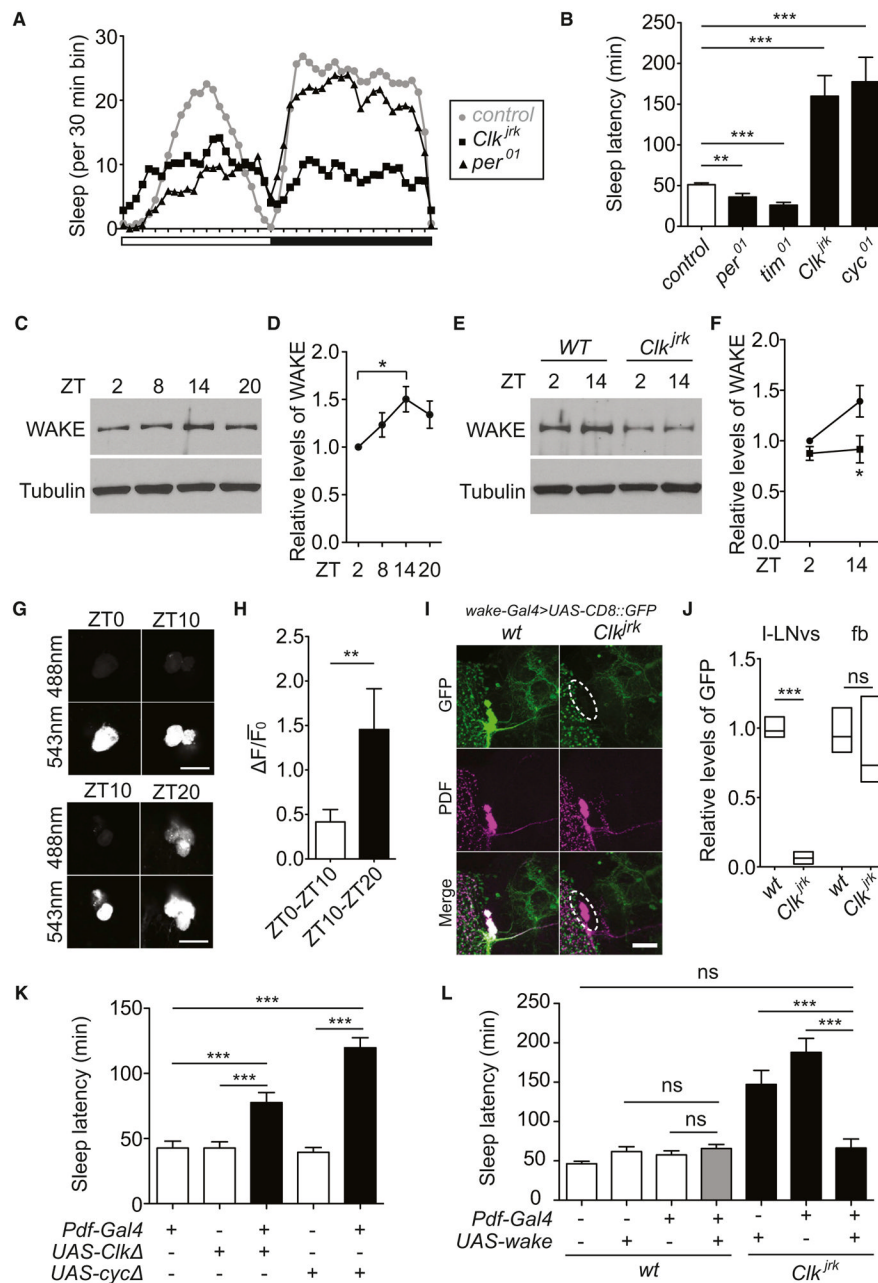
**Figure 4. WAKE Acts Downstream of the Circadian Clock to Regulate Sleep Onset**

(A) Sleep profile of background control (gray circles) (n = 160), $Clk^{jrk}$ (black squares) (n = 63), and $per^{01}$ flies (black triangles) (n = 58), plotted in 30 min bins. White and black bars indicate 12 hr light and dark periods, respectively.

(B) Sleep latency for control (n = 160), $per^{01}$ (n = 58), $tim^{01}$ (n = 41), $Clk^{jrk}$ (n = 63), and $cyc^{01}$ (n = 29) flies.

(C) Western blot using WAKE-Ab1 on wild-type heads at different time points during the day and night.

(D) Relative expression levels of WAKE (n = 7). WAKE expression levels were normalized to ZT2 and Tubulin.

(E) Western blot using WAKE-Ab1 on heads from wild-type (WT) and *Clk^{jrk}* flies at ZT2 and ZT14.

(F) Relative expression levels of WAKE in WT (circles) and *Clk^{jrk}* (squares) flies (n = 6). WAKE expression levels were normalized to ZT2 and Tubulin.

(G) l-LNvs from *wake-Gal4>UAS-kaede* flies were imaged immediately after photoconversion at ZT0 (top) or ZT10 (bottom) and 10 hr after photoconversion. Photoconverted (543 nm) and newly synthesized (488 nm) KAEDE are shown.

(H) Relative amount of de novo KAEDE synthesis within different time windows by normalizing to preexisting red KAEDE ( $\Delta F/\overline{F0}$, n = 8–9 samples).

(I) Whole-mount brain immunostaining of *wake-Gal4 > UAS-CD8::GFP* flies in WT and *Clk^{jrk}* backgrounds with anti-GFP (green) and anti-PDF (magenta). Maximal intensity projections are shown. Dashed lines indicate location of l-LNvs.

(J) Relative levels of GFP signal in l-LNvs and Fan-shaped body (fb) terminals in *wake-Gal4 > UAS-CD8::GFP* flies in WT (n = 9) and *Clk^{jrk}* (n = 9) backgrounds.

(K) Sleep latency for *Pdf-Gal4*/+ (n = 43), *UAS-ClkΔ*/+ (n = 38), *Pdf-Gal4, UAS-ClkΔ*/+ (n = 39), *UAS-CycΔ*/+ (n = 39), and *Pdf-Gal4, UAS-CycΔ*/+ (n = 44) flies.

(L) Sleep latency for wild-type (WT) (n = 88), *UAS-wake/+* (n = 33), *Pdf-Gal4/+* (n = 26), *Pdf-Gal4/UAS-wake* (n = 27), *UAS-wake/+; Clk^{jrk}* (n = 75), *Pdf-Gal4/+; Clk^{jrk}* (n = 78), and *PDF-Gal4, UAS-wake/+; Clk^{jrk}* (n = 79) flies. Scale bar denotes 10 μm in (G) and 50 μm in (I). Mean ± SEM is shown. See also Figure S4.
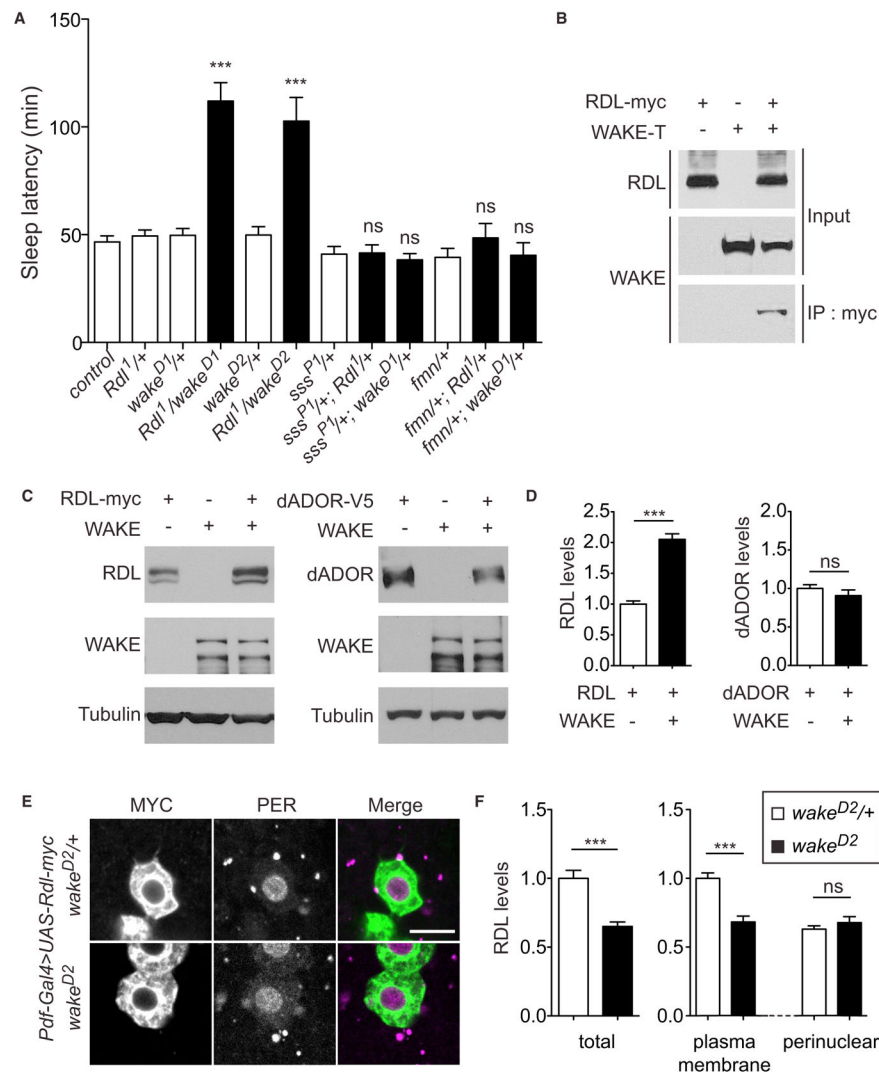
**Figure 5. WAKE Interacts with RDL and Increases RDL Levels**

(A) Dominant (transheterozygous) genetic interactions between *wake* and *Rdl*. Sleep latency for control (n = 130), *Rdl[1]*/+ (n = 82), *wake[D1]*/+ (n = 104), *wake[D1]*/*Rdl[1]* (n = 36), *wake[D2]*/+ (n = 49), *wake[D2]*/*Rdl[1]* (n = 53), *sss[P1]*/+ (n = 54), *sss[P1]*/+; *Rdl[1]*/+ (n = 25), *sss[P1]*/+; *wake[D1]*/+ (n = 36), *fmn*/+ (n = 43), *fmn*/+; *Rdl[1]*/+ (n = 21), and *fmn*/+; *wake[D1]*/+ (n = 12) flies.

(B) Coimmunoprecipitation of WAKE and RDL. Extracts from *Xenopus* oocytes injected with cRNA from *wake-T*, *RDL-myc*, or both were immunoprecipitated with anti-myc antibodies and analyzed by western blotting using WAKE-Ab2 antibodies.

(C) Left: extracts from S2R+ cells transfected with *wake*, *Rdl-myc*, or both were analyzed by western blotting with antibodies against MYC and WAKE (Ab2). Right: extracts from S2R+ cells transfected with *wake*, *dAdoR-V5*, or both were analyzed by western blotting with anti-V5 and WAKE (Ab2) antibodies.

(D) Quantification of RDL (n = 4) or dADOR (n = 3) levels, normalized to Tubulin, from western blot experiments as shown in (C).

(E) Anti-MYC (green) and anti-PER (magenta) immunostaining of l-LNvs in *Pdf-Gal4/+; UAS-Rdl-myc, wake[D2]/+* (top row) and *Pdf-Gal4/+; UAS-Rdl-myc, wake[D2]/ wake[D2]* (bottom row) flies.

(F) Quantification of total (left) and plasma membrane versus perinuclear (right) RDL-MYC levels in the l-LNvs in *wake*$^{D2}$*/+* (n = 9) and *wake*$^{D2}$ (n = 9) backgrounds. Scale bar denotes 10 μm in (E). Mean ± SEM is shown. See also Figure S5.
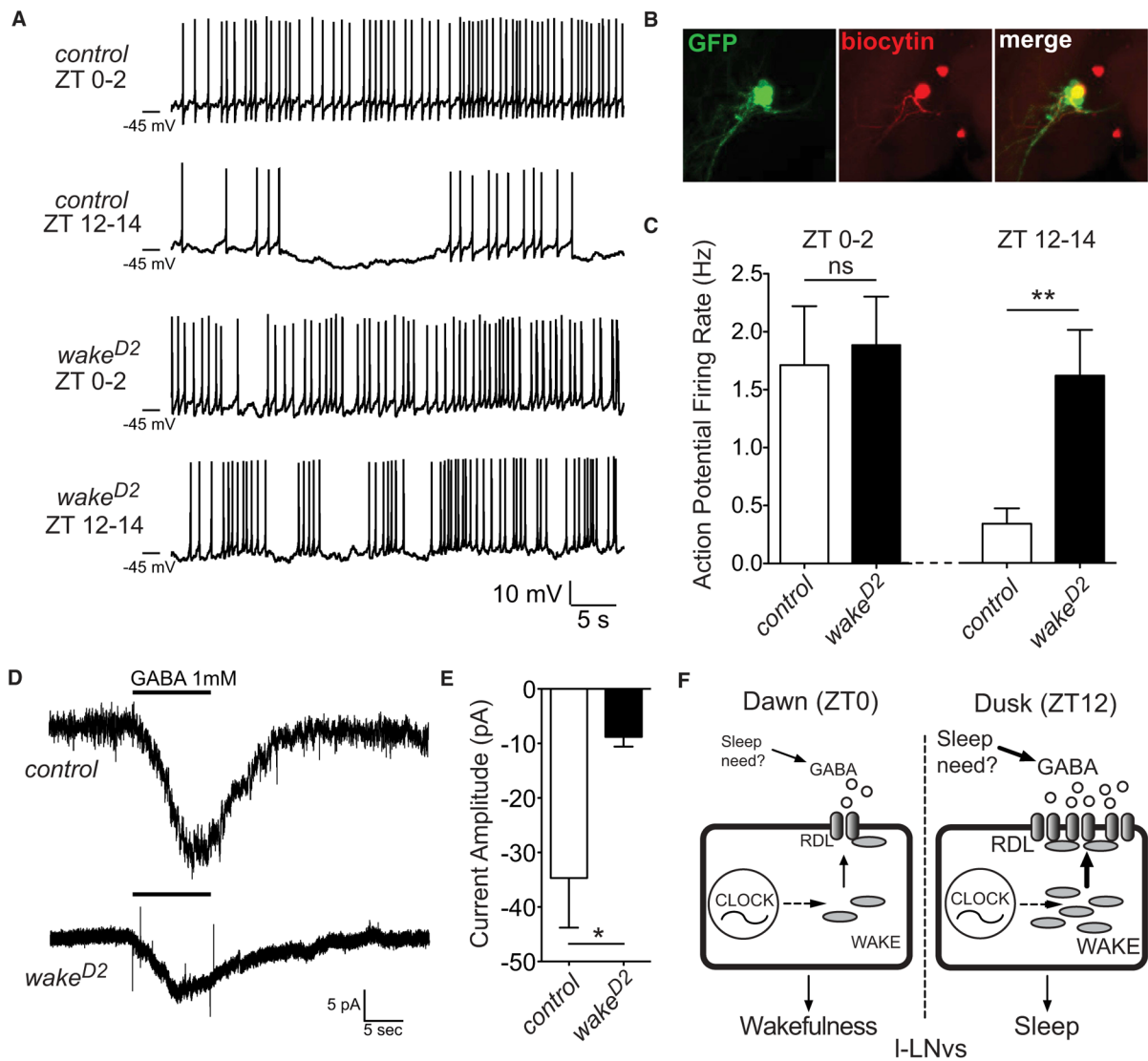
**Figure 6. Excitability Is Increased and GABA Sensitivity Is Decreased in l-LNvs of *wake* Mutants at Dusk**

(A) Representative whole-cell current-clamp recordings of l-LNv neurons in *control* (*Pdf-Gal4/UAS-CD8::GFP*) and *wake[D2]* (*Pdf-Gal4/UAS-CD8::GFP; wake[D2]*) mutant flies at ZT0–ZT2 or ZT12–ZT14.

(B) Immunostaining of a *Pdf-Gal4 > UAS-CD8::GFP* fly brain with a biocytin-filled l-LNv cell.

(C) Quantification of action potential firing rates of *control* flies and *wake[D2]* mutant flies at ZT0–ZT2 or ZT12–ZT14 (n = 8 for each of the 4 groups).

(D) Representative GABA-evoked currents of l-LNvs in *control* (*Pdf-Gal4/UAS-CD8::GFP*) and *wake[D2]* (*Pdf-Gal4/UAS-CD8::GFP; wake[D2]*) mutant flies at ZT11–ZT14. Holding potential is at −70 mV.

(E) Quantification of GABA-evoked currents of l-LNvs from *control* flies (n = 8) and *wake[D2]* flies (n = 6).

(F) Model of WAKE as a molecular intermediary between the circadian clock and sleep. WAKE expression level is regulated by the circadian clock and peaks at dusk (ZT12). At this time, increased WAKE levels upregulate RDL in LNvs and enhance the sensitivity of

these cells to GABA signaling. As a result, the activity of the LNv arousal circuit is inhibited, which facilitates sleep onset in the early night. In contrast, WAKE levels are relatively lower at dawn (ZT0), resulting in less RDL in LNvs at this time. There may also be less GABA signaling to the LNvs at dawn. These factors favor excitation of the LNvs at dawn, promoting wakefulness. The source of GABA signaling is currently unknown and might be regulated by sleep need (see Discussion). Mean ± SEM is shown. See also Figure S6.
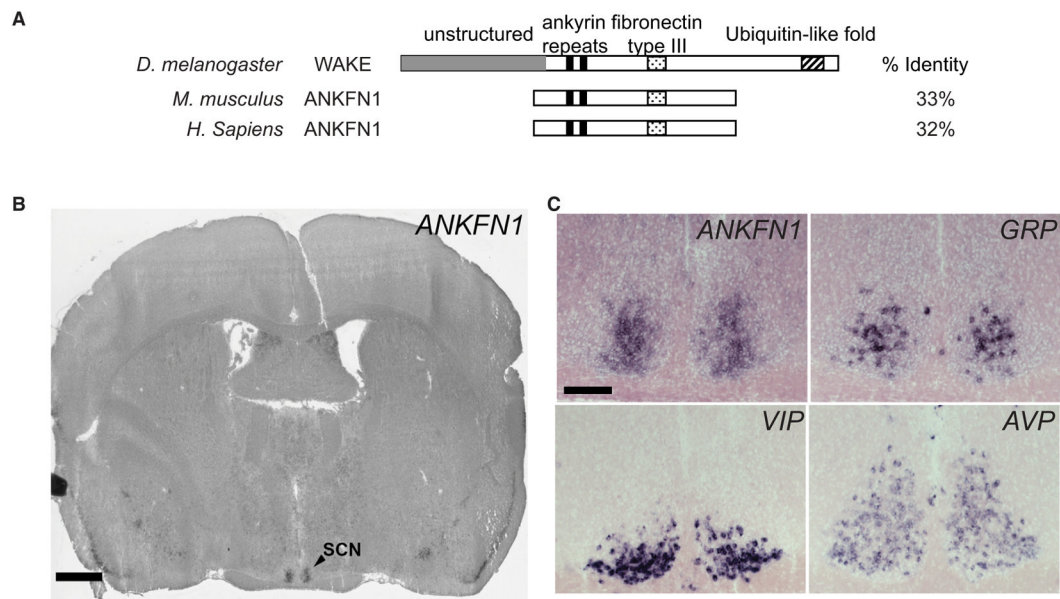
**Figure 7. The Mouse Homolog of WIDE AWAKE Is Expressed in the SCN**

(A) Schematic showing domains of fly WAKE. The ankyrin repeats and fibronectin type III domain are conserved with putative mammalian homologs. Percentage of identity of mouse and human ANKFN1 compared to WAKE is shown.

(B) In situ hybridization of mouse coronal brain section for *ANKFN1*, showing the entire brain. Arrowhead indicates the SCN region; scale bar, ~1 mm.

(C) In situ hybridization of mouse brain sections for *ANKFN1*, *GRP*, *VIP*, and *AVP*, showing selective and robust expression of *Ankfn1* in an SCN subdomain largely overlapping that of *GRP*. Scale bar, 100 µm.